Article

Journal of
Nanoscience and Nanotechnology
Vol. 20, 673–679, 2020
www.aspbs.com/jnn

Effects of Titanium Nano-Foveolae Surfaces on Human Gingival Fibroblasts

Yujun Zhang[1,†], Yilin Zhang[2,†], Tingting Kong[3,4], Bin Ye[5], Xiaoyan Li[1], Ping Ji[1], and Shengjun Sun[1,*]

[1] *Shandong Provincial Key Laboratory of Oral Biomedicine, College of Stomatology, Shandong University, Shandong, 250014, P. R. China*
[2] *Department of Stomatology, Shandong Provincial Hospital Affiliated to Shandong University, Shandong, 250014, P. R. China*
[3] *Key Laboratory of Shanxi Province for Craniofacial Precision Medicine Research, College of Stomatology, Xi'an Jiaotong University, Xi'an, 710000, P. R. China*
[4] *Clinical Research Center of Shanxi Province for Dental and Maxillofacial Diseases, College of Stomatology, Xi'an Jiaotong University, Xi'an, 710000, P. R. China*
[5] *State Key Laboratory of Oral Diseases, West China School of Stomatology, Sichuan University, Sichuan, 610000, P. R. China*

A proper soft tissue seal between implants and gingiva is critical for success of dental implants. Implant surface modification is an important approach for achieving ideal host-implant integration. In this study, we used a new and simple oxidation method to generate a rough surface on implants at the nano scale, which oxidized titanium nano-foveolae (TiNF) surface. We further analyzed the surface topography and tested its effects on biological activities of human gingival fibroblasts. Atomic force microscopy (AFM) and scanning electron microscopy (SEM) examination demonstrated that TiNF disks displayed uniform rough surfaces, with average TiNF diameters of approximately 60 nm and 100 nm respectively. However, the surfaces of smooth samples were highly irregular, and cell adhesion and proliferation rates on TiNF surfaces were significantly higher than those of the smooth surfaces. Extracellular matrix synthesis was also increased in the cells that interacted with oxidized TiNF surfaces. Altogether, these results suggest that the TiNF implant surfaces perform better for human gingival fibroblast biological activities compared to traditional smooth surfaces. Therefore, the TiNF implant surfaces may serve as ideal interface to facilitate implant-host integration.

Keywords: Dental Material, Dental Implants, Titanium, Gingival Fibroblasts.

1. INTRODUCTION

Dental implantation has become one of the best choices for restoring various dentition defects, transforming the lives of people who are edentulous. However, Peri-implantitis due to defective soft tissue sealing remains one of the major cause of implant failure [1, 2]. A successful implant requires not only ideal bone-implant contact and integration but also proper soft tissue seal between the implant and gingiva [3]. A healthy trans-gingival area is therefore very important for inhibiting bacteria from adhering and forming biofilm [4–6]. Therefore, achieving a fast seal is also critical in clinical settings.

It has been reported that surface topography and characteristics of the implant neck affect cell adhesion for soft tissue sealing [7]. Many studies, using a variety of methods, have generated various micro-roughened surfaces and examined the effects of these surfaces on biological characteristics of tissues [8–12]. Contrary to previous beliefs, multiple lines of recent evidence have demonstrated that a micro-roughened surface does not cause increased bacterial plaque, nor does it cause crestal bone tissue loss [13, 14]. Furthermore, a roughened surface facilitates soft tissue attachment compared to traditional smooth surfaces [15, 16]. Therefore, exploring an ideal modified surface for neck implant has become a research priority in the implantation field.

Currently, there are many available state-of-the-art techniques for creating a variety of novel surfaces at the nano scale, including self-assembly of molecule monolayers, nanoparticle deposition and optical methods [17–20]. However, the technical procedures in these reports are complicated and time-consuming, which significantly limits their application. Anodic oxidation is a new and simple method used for generation of a nano-dimension surface by creating a new oxide layer on a titanium implant [21]. Here we used this method to produce a

*Author to whom correspondence should be addressed.
†These two authors contributed equally to this work and should be considered co-first authors.

titanium nano-foveolae (TiNF) structure on the implant surface, and we tested the effects of modified surface on human gingival fibroblast (HGF) activity. Results from the study showed that implant modification with TiNF surfaces profoundly influenced human fibroblast activity and was superior to traditional surfaces for achieving cell attachment and growth.

2. MATERIALS AND METHODS

2.1. Sample Preparation

0.25 nm thick titanium foil was obtained from a commercial firm (Alfa Aesar, American). The anodic oxidation process produced the test samples. Two types of oxidized titanium surfaces were generated (test groups), and one type was produced at a voltage of 25 V in inorganic electrolytes (1 M H_3PO_4, 0.5 wt.% HF, in distilled water) at room temperature (the 25 V group). The other type was produced at a voltage of 40 V in organic electrolytes (0.5 wt% NH_4F, in glycol) at room temperature (the 40 V group). Following anodization, all samples were thoroughly rinsed in distilled water and dried with nitrogen stream. The traditional smooth titanium surfaces were made by machine polishing [22] and served as a control group.

2.2. Surface Topography Characterization

Topographic measurements of titanium surfaces were made by scanning electron microscopy (SEM, JSM-6700F, JEOL, Japan). The 3-dimensional morphology study was performed by atomic force microscopy (AFM, Bioscope II, Digital Instruments, USA). Nanometer scale surface roughness was analyzed using NanoNavi software (ver. 5.00, Japan).

2.3. Cell Culture

Healthy gingival tissues were harvested from the removed teeth of three orthodontic patients. Informed consent was obtained from all patients, and the procedures were approved by the Ethics Committee of Stomatology School of Shandong University. Isolated gingival tissues were cut to cubes of approximately $3 \times 3 \times 3$ mm, placed in 12-well plates, and immobilized with a cover slip. Migrated human gingival fibroblast (HGF) primary cells were harvested, and cultured in Dulbecco's Modified Eagle Medium (DMEM, Hyclone, Logan, UT, USA). Cells were passaged 3 to 5 times and used in all experiments. Sub con?uent HGF cells were seeded onto the smooth and TiNF titanium discs respectively by $1 \times 10^4/cm^2$ in 24-well microplates.

2.4. Cell Morphology

Discs seeded with HGFs were removed from the medium after 4 h culture, and samples were fixed in 2.5% glutaraldehyde in PBS for 1 h at room temperature, rinsed with PBS, and immersed in 0.5 mL of 2% osmium tetroxide for 1 h. After a thorough wash with PBS, the samples were dehydrated in ethanol series, and further dried with supercritical CO_2. Next, the surfaces were sputter-coated with gold and subjected to imaging on a field emission SEM (JSM-6700F, JEOL, Japan) under vacuum.

2.5. Cell Adhesion

Cells cultured on samples at different time points (2 h, 8 h and 24 h respectively) were stained with the LIVE/DEAD® Cell Imaging Kit 488/570 (Thermo Fisher SCIENTIFIC, USA). Live cells were stained green by calcein AM, and dead cells were stained red by EthD-III. After a 30-min incubation with the dyes in the dark, at room temperature, samples were examined with a fluorescence microscope (Leica CTR5000, Leica, Germany). For each sample, five random fields of view were imaged. Software was used to count cells in each photo (Image-Pro Plus 5.0, Media Cybernetics, Silver Spring, MD, USA).

2.6. Cell Proliferation

Cell proliferation of cultured HGFs on different surfaces were analyzed by 3-(4,5-dimethylthiazol-2-yl)-2,5-diphenyl-tetrazolium bromide (MTT, Sigma–Aldrich, St. Louis, MO, USA) assay. Samples from the 3 groups collected after various culture times (1 d, 2 d and 4 d) were cultured in 200 μL DMEM with 20 μL MTT dye agent (5 mg/mL) for 4 h. The culture solutions were then transferred into a 96-multiwell plate for spectrophotometric (Synergy H1, BioTek Instruments, Winooski, VT, USA) analysis.

2.7. Immunofluorescence (IF)

After 24 h of culture, cells were subjected to immunofluorescence for Vinculin (VCL). Specifically, cells were fixed with 4% PFA for 20 min, and blocked with 3% Bovine serum for 20 min. Mouse monoclonal anti-human Vinculin primary antibody (Abcam, Cambridge, MA, USA) was used with 1:200 dilution, as recommended in the manufacturer's datasheet. Sections were inoculated at 4 °C overnight. Red fluorescence-labeled goat anti-mouse secondary antibody (Invitrogen, Carlsbad, CA, USA) was used at a 1:300 dilution for 2 h. After thorough washing, sections were examined under a Leica DM5000B microscope (Leica Microsystems, Wetzlar, Germany).

Table I. Sequences of primers used for RT-qPCR.

Gene	Forward primer (5′–3′)	Reverse primer (5′–3′)
VCL	GTTCACAATGCCCA GAACCT	TCTTTCTAACCCAG CGCAGT
COL1-a1	ACTGGTGAGACCTG CGTGTA	GAATCCATCGGTCA TGCTCT
β-actin	CCTGGCACCCAG CACAAT	GGGCCGGACTCG TCATAC

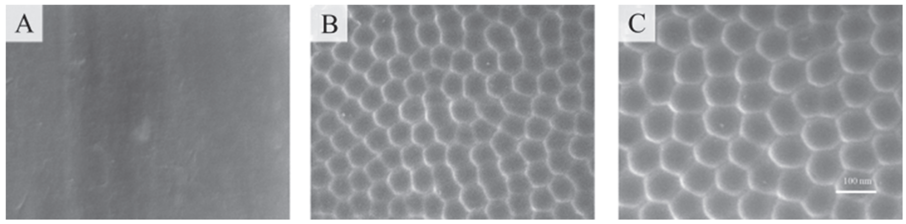

Figure 1. SEM examination of TiNF layer. (A) A sample from the ctrl group showing an irregular and grooved surface. (B) A sample from 25 V group showing an uniformed surface with TiNF diameter of approximately 60 nm. (C) A sample from the 40 V group, showing uniform surface with a TiNF diameter of approximately 100 nm. (Scale bar = 100 nm).

2.8. Real Time Quantitative Polymerase Chain Reaction (RT-qPCR)

Total RNA was extracted using Trizol reagent (Sigma-Aldrich Company, St. Louis, MO, USA) after 1 d, 4 d and 7 d of culture on different surfaces, according to the manufacturer's protocol. Total RNA from the samples were quantified with a spectrophotometer (DU-600, Beckman Instruments, Fullerton, CA, USA). RNA quantification was adjusted to the same level for all samples. The cDNAs were synthesized using a Real-time PCR kit (Takara, Japan). Real-time PCR analyses were carried out to evaluate the expression of VCL and COL-a1 (Table I) using a SYBR Green kit. Gene expression was analyzed using the $2^{-\Delta\Delta Ct}$ method. The tests were carried out and analyzed using a Real-time PCR System (Applied Biosystems Viia7, Life Technologies Corporation, Carlsbad, CA, USA).

2.9. Enzyme-Linked Immunosorbent Assay (ELISA)

The HGFs on each sample were collected, and the amount of Fibronectin 1 (FN-1) release was detected and analyzed using an ELISA kit (R&D Systems Inc., Minneapolis, MN, USA) after culture for 1 d, 4 d and 7 d, following the manufacturer's protocol. The optical densities were determined at a 595-nm reference wavelength at the end of the ELISA protocol, and normalized to cell number, using a spectrophotometer (Synergy H1, BioTek Instruments, Winooski, VT, USA). Standards supplied in the kit were used to make calibration curves.

2.10. Statistical Analysis

One-way ANOVA and Student-Newman-Keuls post hoc test were used with SPSS software (SPSS 14, SPSS, Chicago, IL, USA) to compare differences between groups. P value <0.05 was considered statistically significant.

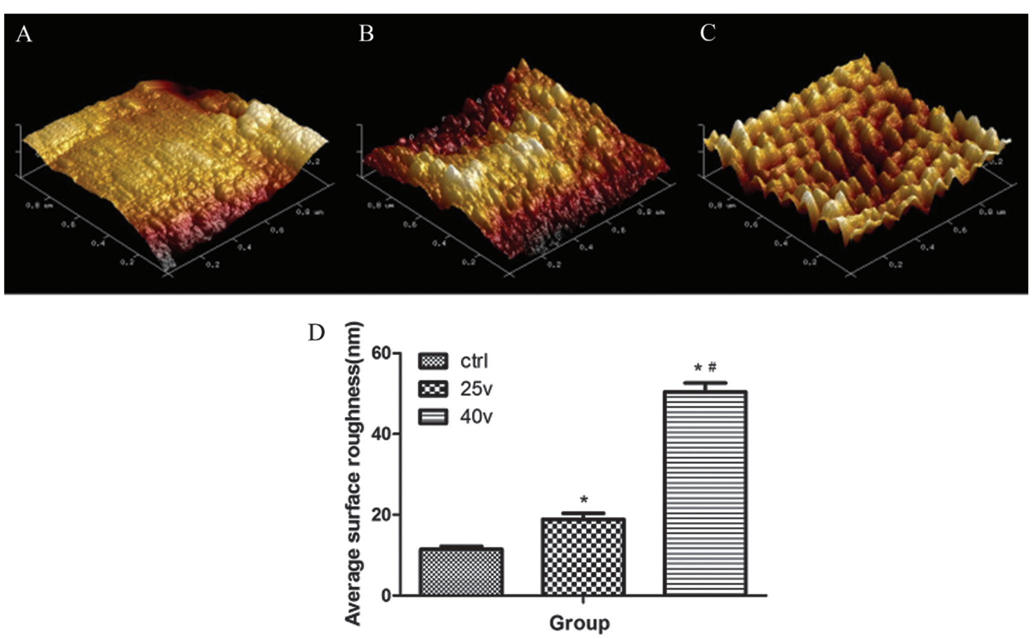

Figure 2. AFM examination of TiNF layer. (A) A sample from the ctrl group showing an irregular surface. (B) A sample from the 25 V group showing uniform surface. (C) A sample from the 40 V group showing a uniform but rough surface. (D) The average surface roughness for three groups, showing significant differences between ctrl and oxidized titanium samples. The 40 V group had the highest roughness, followed by the 25 V group. (*, $P < 0.05$ compared with Ctrl group; #, $P < 0.05$ compared with 25 V group).

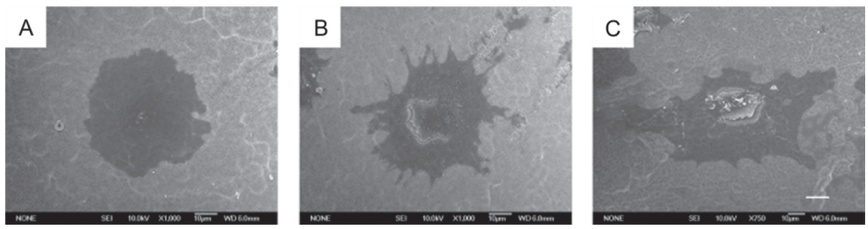

Figure 3. SEM examination of attached cells on TiNF layers after 4 h of culture. (A) Ctrl group, (B) 25 V group, and (C) 40 V group. Note, cells on TiNF layer display more obvious cell filopodia formation than the Ctrl group. (Scale bar = 10 μm).

3. RESULTS

3.1. Surface Modification and Characterization

Three different types of titanium surfaces were generated using the above-mentioned techniques: smooth titanium surfaces (Ctrl group) and two types of oxidized titanium surfaces (25 V and 40 V group). We first characterized the manufactured surfaces by SEM. Results from this study showed that the surfaces of three types of samples were dramatically different (Figs. 1(A–C)). The oxidized disks displayed uniform rough surfaces, with average TiNF diameters of approximately 60 and 100 nm respectively (Figs. 1(B, C)). By contrast, the smooth samples showed grooved surfaces (Fig. 1(A)).

AFM analysis showed that the mean nanometer scale surface roughness for the oxidized samples was significantly higher than that of smooth ones. (Figs. 2(A–C)), and the 40 V group displayed highest roughness among three types of samples, followed by the 25 V group (Fig. 2(D)).

3.2. Cell Morphology, Adhesion, and Proliferation

The morphology of HGFs attached to smooth titanium surfaces and oxidized titanium surfaces were then studied by SEM (Fig. 3). TiNF cells exhibited elegant filopodia after 4 h of culture, suggesting the biologically active status of HGFs. In contrast, cells from the control group failed to form obvious filopodia, and their cytoplasm appeared condensed.

Cell adhesion and proliferation on modified surfaces were examined. HGFs were cultured on different surfaces for 2 h, 8 h and 24 h, and the numbers of attached cells on each surface were counted and compared among the three groups. The results showed that the cell numbers on the oxidized surfaces were significantly higher than on smooth surfaces at all the time points examined (Fig. 4).

MTT assays for cell proliferation were performed after 1 d, 2 d and 4 d of culture. Markedly greater values, representing higher numbers of adherent cells, were detected for the TiNF surfaces than for smooth surfaces on d 1, and these values increased in a time-dependent

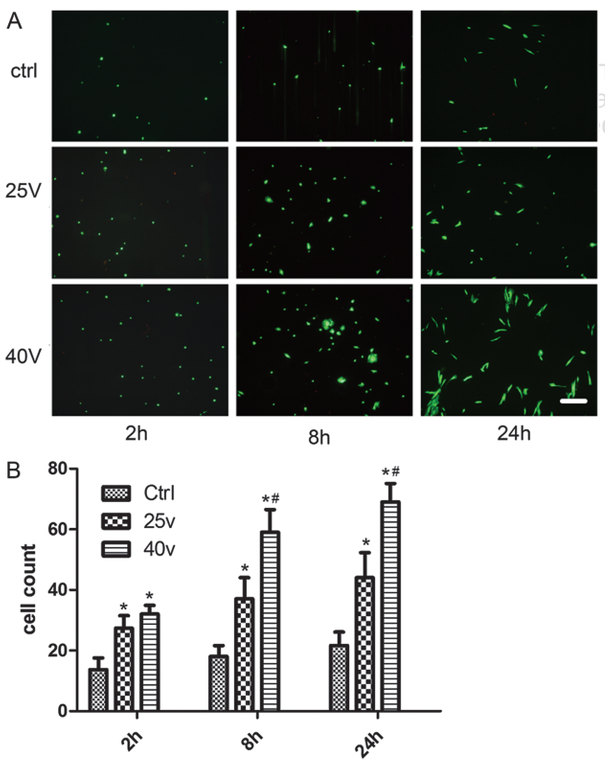

Figure 4. Viability/cytotoxicity assay. (A) HGFs cultured on 3 different surfaces at 3 different time points. Live cells were stained green by calcein AM. (B) The cell numbers in the 25 V and 40 V groups were significantly higher than the Ctrl group at all time points examined (*, $P < 0.05$ compared with Ctrl group; #, $P < 0.05$ compared with 25 V group. Scale bar = 100 μm).

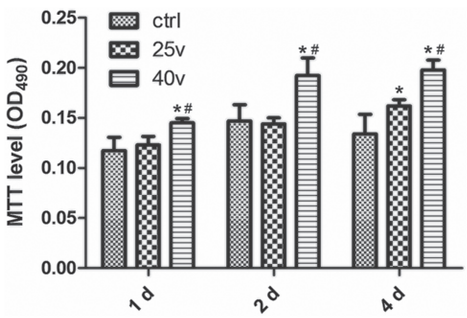

Figure 5. MTT assay of HGFs after 1 d, 2 d and 4 d of culture. Higher values were seen in the 25 V and 40 V groups than in the smooth ones, and these values increased with time (*, $P < 0.05$ compared with ctrl group; #, $P < 0.05$ compared with 25 V group).

manner (Fig. 5). Altogether, these results suggest that HGFs attach and grow better on oxidized surfaces than on smooth surfaces.

3.3. Expression of ECM Synthesis Markers

Finally, the expression of VCL and COL-a1 in HGFs was examined by IF and RT-qPCR, and FN expression was examined by ELISA. Taken together, these genes and proteins are markers for ECM synthesis of fibroblasts. The results showed that expression levels of VCL and COL-a1 of HGFs were significantly elevated on roughened surfaces compared to smooth surfaces after 4 d of culture (Figs. 6(A, B)). Additionally, we observed that, VCL expression levels in the TiNF group were significantly

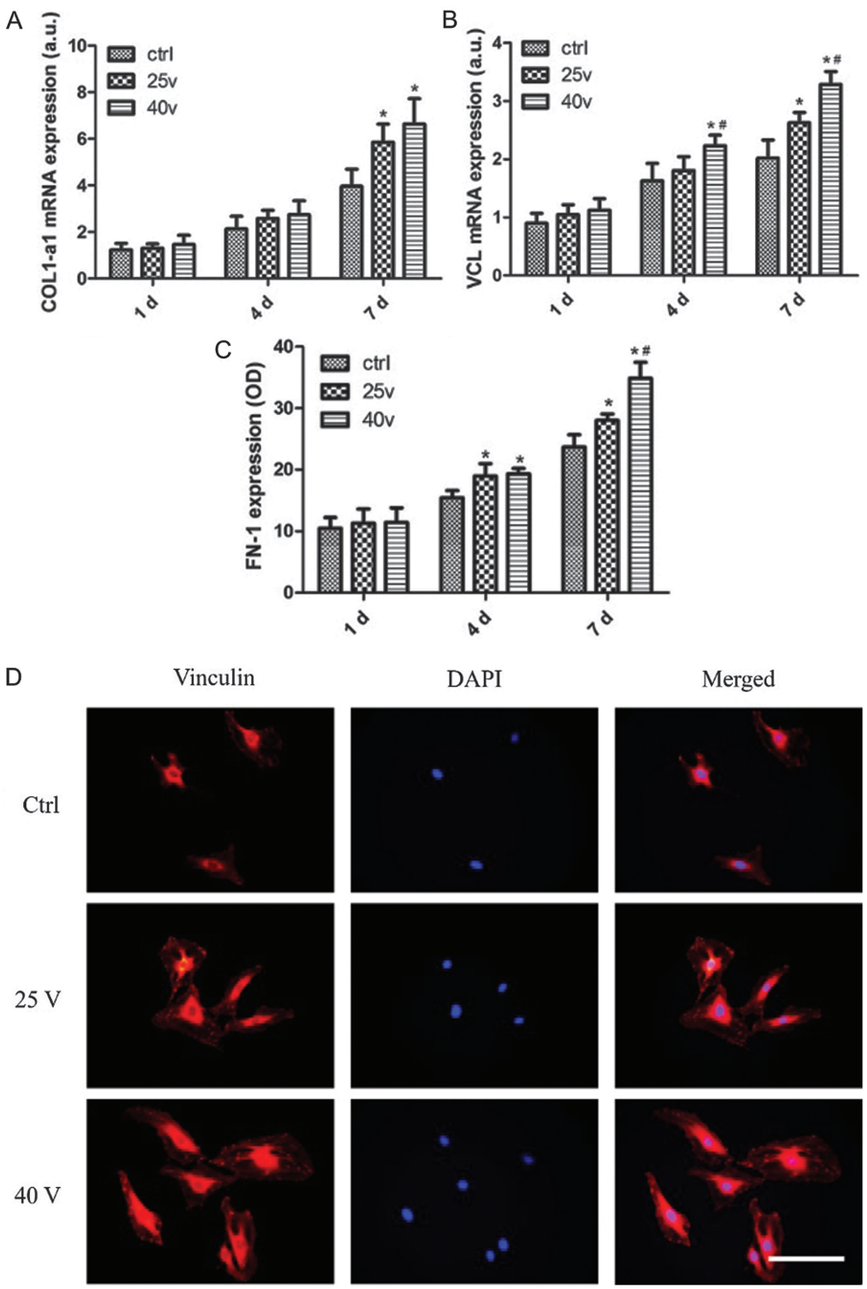

Figure 6. RT-qPCR, ELISA and IF assay for HGFs on different surfaces. (A) COL-a1 mRNA expression levels were significantly elevated after 7 d of culture. (B) Expression levels of VCL mRNA were also significantly elevated in the 25 V and 40 V groups, compared to the ctrl group after 4 d in culture. (C) ELISA assays for HGFs after 1 d, 4 d and 7 d of culture. Levels of FN were increased in the 25 V and 40 V groups compared to the ctrl group after 4 d and 7 d of culture. The FN level in the 40 V group was also higher than the 25 V group after 7 d. (D) IF staining of VCL at 24 h (*, $P < 0.05$ compared with ctrl group; #, $P < 0.05$ compared with 25 V group. Scale bar = 100 μm).

increased at 24 h, and located at focal adhesion sites (Fig. 6(D)). Similarly, the expression levels of FN were also increased on TiNF surfaces compared to smooth surfaces after 4 d and 7 d of culture (Fig. 6(C)). Altogether, these results indicate that the titanium surface variation affects gene expression in HGFs.

4. DISCUSSION

Many dental implant surface modification methods are now available to change the surface roughness at the nanometer scale, thus enhancing the surface affinity for host tissues. In addition to bone-implant integration, proper soft tissue attachment to the implant is also critical for successful implantation [23]. Nano structuring technology is a very effective method to enhance the performance of titanium implants [24, 25]. Nanostructured materials possess enlarged surface area; therefore, these materials present an ideal surface-tissue interface for the implants [26, 27]. It was reported that nano crystallization of Ti materials can create a biomimetic relationship with host tissues through simulation of natural cellular environments at nanometer-scale hierarchy [28]. In this study, we showed a new approach to enhance the integration between gingival tissue and dental implant neck by fabricating a nanoscale TiNF surface on the implant through anodic oxidation. We characterized the TiNF of oxidized titanium implant surfaces by SEM and AFM, and further investigated the effects of such surface on HGF adhesion, proliferation and ECM synthesis.

Our surface topography data demonstrated that the nano-roughness of the surfaces increased with presence of nanostructures. Under SEM, uniform TiNF surfaces of oxidized disks were clearly observed, whereas the smooth samples exhibited irregular surface grooves. The diameters of TiNF, generated under different voltages were also different, and the diameter increased as the voltage increased. The mean nanometer scale surface roughness was significantly higher for oxidized surfaces than smooth ones. These results are consistent with a previous report [29].

Our further surface-tissue interaction analysis used HGFs as major resident cells to investigate peri-implant connective attachment. This analysis demonstrated that the rough surface indeed performed better in supporting cell adhesion and growth. Compared with surfaces, more HGFs adhered to the oxidized TiNF surfaces, as evidenced by Live/Dead cell detection. The results suggest that the nano-rough surface facilitates initial cell adhesion, which is the key step to establishing the tissue-implant connection.

Altogether, these data show that the rough surfaces of TiNF promoted cell growth and differentiation compared to smooth surfaces. The TiNF surfaces therefore serve as a better interface for cell activity in the peri-implant area, and may potentially facilitate establishment of tissue-implant connection. Further *in vivo* testing will be performed in future studies.

5. CONCLUSIONS

In conclusion, we provided a new approach for surface modification of transmucosal area of dental implants. We demonstrated that the anodic oxidized TiNF implant surface significantly promotes biological activities of HGFs in comparison to traditional smooth surfaces. These results also indicate that this type new surface may facilitate soft tissue adhesion at the implant-host interface, which is worth pursuing in further research.

Acknowledgments: This research was supported by The Fundamental Research Funds of Shandong University (21350073614072), the Shandong Provincial Natural Science Foundation (ZR2017BH030) and the Young Scholars Program of Shandong University (2018WLJH79).

References and Notes

1. Al-Radha, A.S., Pal, A., Pettemerides, A.P. and Jenkinson, H.F., **2012**. Molecular analysis of microbiota associated with peri-implant diseases. *Journal of Dentistry*, *40*(11), pp.989–998.
2. Barbour, M.E., O'Sullivan, D.J., Jenkinson, H.F. and Jagger, D.C., **2007**. The effects of polishing methods on surface morphology, roughness and bacterial colonisation of titanium abutments. *Journal of Materials Science: Materials in Medicine*, *18*(7), pp.1439–1447.
3. Cranin, A.N., Baraoidan, M. and DeGrado, J., **1997**. A human clinical and histologic report of an osseointegrated titanium alloy root form implant. *Journal of Oral Implantology*, *23*(1), pp.21–24.
4. Abdulmajeed, A.A., Willberg, J., Syrjanen, S., Vallittu, P.K. and Narhi, T.O., **2015**. *In vitro* assessment of the soft tissue/implant interface using porcine gingival explants. *Journal of Materials Science: Materials in Medicine*, *26*(1), pp.5385–5392.
5. Rutkunas, V., Bukelskiene, V., Sabaliauskas, V., Balciunas, E., Malinauskas, M. and Baltriukiene, D., **2015**. Assessment of human gingival fibroblast interaction with dental implant abutment materials. *Journal of Materials Science: Materials in Medicine*, *26*(4), pp.169–178.
6. Watkins, A.J., Pearce, G., Unak, P., Guldu, O.K., Yasakci, V., Akin, O., Aras, O., Wong, J. and Ma, X., **2018**. Tissue morphology and gene expression characterisation of transplantable adenocarcinoma bearing mice exposed to fluorodeoxyglucose-conjugated magnetic nanoparticles. *Journal of Biomedical Nanotechnology*, *14*(11), pp.1979–1991.
7. Diener, A., Nebe, B., Luthen, F., Becker, P., Beck, U., Neumann, H.G. and Rychly, J., **2005**. Control of focal adhesion dynamics by material surface characteristics. *Biomaterials*, *26*(4), pp.383–392.
8. Zhang, Q., Lin, S., Shi, S., Zhang, T., Ma, Q., Tian, T., Zhou, T., Cai, X. and Lin, Y., **2018**. Anti-inflammatory and antioxidative effects of tetrahedral DNA nanostructures via the modulation of macrophage responses. *ACS Applied Materials & Interfaces*, *10*(4), pp.3421–3430.
9. Xu, H.H., Wang, P., Wang, L., Bao, C., Chen, Q., Weir, M.D., Chow, L.C., Zhao, L., Zhou, X. and Reynolds, M.A., **2017**. Calcium phosphate cements for bone engineering and their biological properties. *Bone Research*, *5*, pp.17056–17075.
10. Xing, W.R., Goodluck, H., Zeng, C. and Mohan, S., **2017**. Role and mechanism of action of leucine-rich repeat kinase 1 in bone. *Bone Research*, *5*, pp.17003–17016.
11. Tian, T., Liao, J., Zhou, T., Lin, S., Zhang, T., Shi, S.R., Cai, X. and Lin, Y., **2017**. Fabrication of calcium phosphate microflowers and their extended application in bone regeneration. *ACS Applied Materials & Interfaces*, *9*(36), pp.30437–30447.

12. Liu, M., Zeng, X., Ma, C., Yi, H., Ali, Z., Mou, X., Li, S., Deng, Y. and He, N., **2017**. Injectable hydrogels for cartilage and bone tissue engineering. *Bone Research*, *5*, p.17014.
13. Kramer, P.R., Janikkeith, A., Cai, Z., Ma, S. and Watanabe, I., **2009**. Integrin mediated attachment of periodontal ligament to titanium surfaces. *Dental Materials*, *25*(7), pp.877–883.
14. Kononen, M., Hormia, M., Kivilahti, J., Hautaniemi, J. and Thesleff, I., **1992**. Effect of surface processing on the attachment, orientation, and proliferation of human gingival fibroblasts on titanium. *Journal of Biomedical Materials Research*, *26*(10), pp.1325–1341.
15. Novaes, A.B., Jr., de Oliveira, R.R., Muglia, V.A., Papalexiou, V. and Taba, M., **2006**. The effects of interimplant distances on papilla formation and crestal resorption in implants with a morse cone connection and a platform switch: A histomorphometric study in dogs. *Journal of Periodontology*, *77*(11), pp.1839–1849.
16. Glauser, R., Schupbach, P., Gottlow, J. and Hammerle, C.H., **2005**. Periimplant soft tissue barrier at experimental one-piece mini-implants with different surface topography in humans: A light-microscopic overview and histometric analysis. *Clinical Implant Dentistry and Related Research*, *7*(Suppl 1), pp.S44-S51.
17. Yang, W.F., Long, L., Wang, R., Chen, D., Duan, S. and Xu, F.J. **2018**. Surface-modified hydroxyapatite nanoparticle-reinforced polylactides for three-dimensional printed bone tissue engineering scaffolds. *Journal of Biomedical Nanotechnology*, *14*(2), pp.294–303.
18. Sun, S., Yu, W., Zhang, Y. and Zhang, F., **2013**. Increased pre-osteoblast adhesion and osteogenic gene expression on TiO_2 nanotubes modified with KRSR. *Journal of Materials Science: Materials in Medicine*, *24*(4), pp.1079–1091.
19. Pachauri, P., Bathala, L.R. and Sangur, R., **2014**. Techniques for dental implant nanosurface modifications. *Journal of Advanced Prosthodontics*, *6*(6), pp.498–504.
20. Li, Q., Zhao, D., Shao, X., Lin, S., Xie, X., Liu, M., Ma, W., Shi, S. and Lin, Y., **2017**. Aptamer-modified tetrahedral DNA nanostructure for tumor-targeted drug delivery. *ACS Applied Materials & Interfaces*, *9*(42), pp.36695–36701.
21. Wennerberg, A. and Albrektsson, T., **2009**. Effects of titanium surface topography on bone integration: A systematic review. *Clinical Oral Implants Research*, *20*(Suppl 4), pp.172–184.
22. Anselme, K. and Bigerelle, M., **2005**. Topography effects of pure titanium substrates on human osteoblast long-term adhesion. *Acta Biomaterialia*, *1*(2), pp.211–222.
23. Cai, X., Xie, J., Yao, Y., Cun, X., Lin, S., Tian, T., Zhu, B. and Lin, Y., **2017**. Angiogenesis in a 3D model containing adipose tissue stem cells and endothelial cells is mediated by canonical WNT signaling. *Bone Research*, *5*, pp.17048–17061.
24. Yi, H., Ur Rehman, F., Zhao, C., Liu, B. and He, N., **2016**. Recent advances in nano scaffolds for bone repair. *Bone Research*, *4*, pp.16050–16061.
25. Liao, J., Tian, T., Shi, S., Xie, X., Ma, Q., Li, G. and Lin, Y. **2017**. The fabrication of biomimetic biphasic CAN-PAC hydrogel with a seamless interfacial layer applied in osteochondral defect repair. *Bone Research*, *5*, pp.17018–17033.
26. Tian, T., Zhang, T., Zhou, T., Lin, S., Shi, S. and Lin, Y., **2017**. Synthesis of an ethyleneimine/tetrahedral DNA nanostructure complex and its potential application as a multi-functional delivery vehicle. *Nanoscale*, *9*(46), pp.18402–18412.
27. Meirelles, L., Arvidsson, A., Albrektsson, T. and Wennerberg, A. **2007**. Increased bone formation to unstable nano rough titanium implants. *Clinical Oral Implants Research*, *18*(3), pp.326–332.
28. Rahman, S., Gulati, K., Kogawa, M., Atkins, G.J., Pivonka, P., Findlay, D.M. and Losic, D., **2016**. Drug diffusion, integration, and stability of nanoengineered drug-releasing implants in bone *ex-vivo*. *Journal of Biomedical Materials Research Part A*, *104*(3), pp.714–725.
29. Yu, W.Q., Xu, L. and Zhang, F.Q., **2014**. The effect of Ti anodized nano-foveolae structure on preosteoblast growth and osteogenic gene expression. *Journal for Nanoscience and Nanotechnology*, *14*(6), pp.4387–4393.

Received: 8 July 2017. Accepted: 26 January 2019.